Crystal Structure of Selenosubtilisin at 2.0-Å Resolution[†,‡]

Rashid Syed, Zhen-Ping Wu,[§] James M. Hogle,[∥] and Donald Hilvert*

Departments of Chemistry and Molecular Biology, The Scripps Research Institute, 10666 North Torrey Pines Road, La Jolla, California 92037

Received December 4, 1992; Revised Manuscript Received March 23, 1993

ABSTRACT: The three-dimensional structure of selenosubtilisin, an artificial selenoenzyme, has been solved at 2.0-Å resolution by the method of molecular replacement. Selenosubtilisin is a chemical derivative of the bacterial serine protease subtilisin in which the catalytically essential serine residue has been replaced with a selenocysteine. Its unique hydrolytic and redox properties reflect the intrinsic chemical reactivity of the selenium prosthetic group. Structural analysis of the modified protein reveals that the selenium moiety is selectively incorporated into the side chain of residue 221 and confirms the seleninic acid oxidation state expected from treatment of the enzyme with hydrogen peroxide prior to crystallization. Although the seleninic acid replaces the essential nucleophile in the enzyme's catalytic triad and introduces a negative charge into the active site, the interaction between His64 and Asp32 is not altered by the modification. Hydrogen bonds from the oxygen atoms of the seleninic acid to His64 and to Asn155 in the oxyanion hole confine the prosthetic group to a single well-defined conformation within the active site. These interactions thus provide a structural basis for understanding the seleninic acid's unusually low pK_a, the enzyme's relatively sluggish rate of reaction with thiols, and its much more efficient peroxidase activity. Aside from the active site region, the structure of the protein is essentially the same as that previously reported for native subtilisin Carlsberg, indicating the viability of chemical modification strategies for incorporating site-specific changes into the protein backbone. Comparison of the three-dimensional structures of selenosubtilisin and glutathione peroxidase, an important naturally occurring selenoenzyme, provides the means to evaluate how the function of the selenium prosthetic group varies with molecular context.

Site-specific modification of proteins is a valuable strategy for probing structure–function relationships and for engineering new catalytic activities into enzyme active sites. The bacterial serine protease subtilisin (EC 3.4.21.14) has proven to be a particularly useful model in this regard (Wells & Estell, 1988). It has been extensively mutagenized to improve its stability, to alter its pH–rate profile and substrate selectivity, and to probe its mechanism of action. Because the enzyme can be crystallized readily, high-resolution X-ray structures are also available for several subtilisin variants.

We recently prepared selenosubtilisin, a chemical derivative of subtilisin Carlsberg in which the catalytically essential serine residue is replaced by selenocysteine (Ser221Sec)[1] (Wu & Hilvert, 1989). The analogous cysteine variant (Ser221Cys) has been known for several years [for a review, see Philipp and Bender (1983)], and comparison of the properties of the OH, SH, and SeH enzymes has shed light on the relative importance of steric over electronic factors in catalysis. While both thiol- and selenosubtilisin are poor peptidases, they each catalyze the hydrolysis of activated acyl derivatives by a two-step mechanism involving formation of a transient acyl-enzyme intermediate. The latter is efficiently trapped by amines, which has led to practical applications of thiolsubtilisin as a catalyst for the synthesis of peptides by segment condensation (Nakatsuka et al., 1987). Thiolsubtilisin's efficiency as a peptide ligase was recently enhanced further by mutating a second residue in the active site to relieve steric crowding (Abrahmsén et al., 1991). Because partitioning of selenosubtilisin's acyl-enzyme intermediate toward aminolysis over hydrolysis is even more favorable than that observed for thiolsubtilisin (Wu & Hilvert, 1989), it may eventually prove to be a superior catalyst for acyl-transfer reactions.

In addition to its hydrolytic properties, selenosubtilisin exhibits significant redox activity, catalyzing the reduction of hydrogen peroxide and alkyl hydroperoxides with concomitant oxidation of thiols (Wu & Hilvert, 1990; Bell et al., 1993). In this regard it mimics the naturally occurring selenoenzyme glutathione peroxidase (EC1.11.1.9), which plays an important role in the defense of mammalian cells, protecting lipid membranes and other cellular components against oxidative damage (Wendel, 1980; Ladenstein, 1984). Glutathione peroxidase is an unusually efficient enzyme, operating close to the diffusion limit. Its kinetic mechanism has been proposed to involve interconversion of selenol (ESeH), selenenic acid (ESeOH), and selenenyl sulfide (ESeSR) intermediates (Scheme I). A seleninic acid derivative ($ESeO_2H$) can also be formed in the presence of high concentrations of hydroperoxide, but it is believed to lie off the main catalytic pathway. The available data on selenosubtilisin suggest that it functions in a manner similar to that of the natural peroxidase. Seleninic acid, selenenyl sulfide, and selenolate forms of the semisynthetic enzyme have been isolated and characterized by ^{77}Se-NMR spectroscopy (House et al., 1992). Each of these is competent in the peroxidase reaction, although reactions initiated by the seleninic acid show an initial lag phase that

[†] This work was supported in part by a grant from the National Science Foundation (CHE-8917559), a postdoctoral fellowship to R.S. from the Department of Health of Human Services (T32A107244), and a postdoctoral fellowship to Z.-P.W. from the California Affiliate of the American Heart Association. D.H. is a Fellow of the Alfred P. Sloan Foundation.

[‡] The crystallographic coordinates have been deposited in the Brookhaven Protein Data Bank under the file name 1SEL.

* Address correspondence to this author.

[§] Current address: SYVA Co., Palo Alto, CA 94303.

[∥] Current address: Department of Biological Chemistry and Molecular Pharmacology, Harvard Medical School, Boston, MA 02115.

[1] Abbreviations: DTT, dithiothreitol; NMR, nuclear magnetic resonance; PEG, poly(ethylene glycol); PIPES, 1,4-piperazinebis(ethanesulfonic acid); Sec, selenocysteine.

0006-2960/93/0432-6157$04.00/0

Scheme I

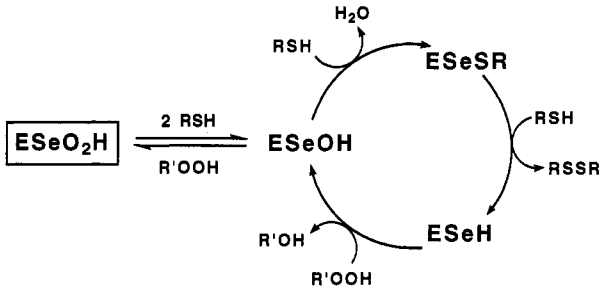

is not observed with the other derivatives (Bell et al., 1993). Presumably, this species must first be reduced to the selenenic acid to access the most efficient catalytic cycle. The fact that ping-pong kinetics are seen under steady-state conditions is consistent with the intermediacy of one or more covalent enzyme adducts during catalysis (Wu & Hilvert, 1989; Bell et al., 1993).

There are also a number of notable differences between glutathione peroxidase and selenosubtilisin. While both enzymes reduce a variety of hydroperoxides to the corresponding alcohols (Günzler et al., 1972; Bell et al., 1993; Z.-P. Wu, unpublished results), the choice of reductant is more restricted. In the case of the naturally occurring enzyme, glutathione and structurally related thiols are the most efficient donor substrates: for example, glutathione is utilized ca. 10^2 times more efficiently than mercaptoethanol for the reduction of hydrogen peroxide (Flohé et al., 1971). In contrast, glutathione and other alkyl thiols are relatively poor substrates for selenosubtilisin, which preferentially employs the aromatic donor 3-carboxy-4-nitrobenzenethiol (Bell et al., 1993). Although its substrate specificity has not been fully optimized, it is apparent that even with an aromatic thiol selenosubtilisin is considerably less efficient than the natural enzyme. Because the pH–rate profiles of the two systems differ (the rates of selenosubtilisin-catalyzed reactions increase with decreasing pH, while those of glutathione peroxidase are maximal at pH 8.8), a direct comparison is difficult to make. However, at their respective optima, we estimate that the natural selenoenzyme is roughly 10^5 times more efficient than the semisynthetic catalyst for reduction of alkyl hydroperoxides (Bell et al., 1993).

Structural differences between the two enzymes presumably underlie their individual substrate specificities and catalytic efficiencies. Glutathione peroxidase is a tetramer of four identical subunits (M_r 21 000), while selenosubtilisin is a monomeric protein (M_r 27 000). The crystal structure of glutathione peroxidase at 2.0-Å resolution shows that the enzyme's active sites are located in shallow depressions on the protein surface (Epp et al., 1983). The catalytically essential selenocysteine residues (Sec45) are thus readily accessible to solvent and solvent-associated molecules. Moreover, there are relatively few residues within 5 Å of the selenocysteine moiety that could stabilize its various oxidation states or participate in catalysis. In contrast, the selenium prosthetic group of selenosubtilisin is expected to be embedded in a well-defined binding pocket as part of a catalytic triad consisting of residues His64 and Asp32. Structural studies of unmodified subtilisins suggest further that the oxyanion hole formation by the side-chain amide of Asn155 and the backbone amide of residue 221 might contribute to the stabilization of anionic selenium derivatives [see, for example, Robertus et al. (1972) and Matthews et al. (1975)]. To verify these suppositions and to assess how structural context modulates the intrinsic reactivity of the selenium prosthetic group, high-resolution data on selenosubtilisin are required. This information is also necessary for efforts to design improved substrates for the enzyme and to optimize its catalytic efficiency through additional site-specific changes within the active site. We have consequently initiated detailed studies of the artificial peroxidase and report herein its three-dimensional structure at 2.0-Å resolution.

Table I: Data Collection Statistics

resolution range (Å)	possible reflections	reflections collected	av $\langle I/\sigma(I)\rangle$	R_{sym}[a]
40.0–3.63	5735	5573	63.7	0.066
3.63–2.88	5662	5505	23.9	0.091
2.88–2.52	5592	5172	9.6	0.145
2.52–2.29	5625	4757	5.7	0.176
2.29–2.13	5569	3865	3.4	0.213
2.13–2.00	5618	2636	1.9	0.243

[a] $R_{sym} = \Sigma|I_{obs} - I_{av}|/\Sigma I_{av}$.

MATERIALS AND METHODS

Selenosubtilisin. Selenosubtilisin was prepared and purifed as described previously using subtilisin Carlsberg as the template for chemical modification (Bell et al., 1993). The seleninic acid form of the enzyme was obtained by dialyzing the protein sequentially against 20 mM dithiothreitol (DTT) and 20 mM H_2O_2 and then exhaustively against buffer alone [10 mM 1,4-piperazinebis(ethanesulfonic acid) (PIPES) and 10 mM $CaCl_2$, pH 7.0].

Crystallization. Crystals of selenosubtilisin (0.5 mm × 0.3 mm × 0.1 mm) were grown at 22.5 °C in 16–20% poly(ethylene glycol) (PEG) 8000 buffered with 0.2 M imidazole–malate (pH 8.0) at a protein concentration of 15 mg/mL by the sitting drop vapor diffusion method. The crystals belong to the monoclinic space group $P2_1$, with a = 75.8 Å, b = 65.4 Å, c = 53.3 Å, and β = 107.3°. The volume per unit molecular mass (V_m) is 2.43 Å^3/Da (Matthews, 1968). This value corresponds to a crystallographic asymmetric unit containing two molecules of selenosubtilisin (M_r 27 384) and a solvent content of 49%.

Data Collection. Single crystals were mounted in quartz capillaries, and X-ray diffraction data were collected with a Siemens multiwire area detector using Cu Kα radiation from an Enraf-Nonius GX-18 rotating anode generator operated at 40 kV, 55 mA, with a 100-μm focus and Franks mirror optics. The data set (94% complete to 2.5 Å and 75% complete to 2.0 Å) was collected from two crystals. The raw data were processed using the XENGEN software package (Howard et al., 1987). Statistics for the merged three-dimensional data are presented in Table I.

Structure Determination. The structure was solved by molecular replacement using the MERLOT suite of programs (Fitzgerald, 1988) with data from 8.0- to 4.0-Å resolution. The orientation of the two molecules was determined by computing cross-rotation functions based on the previously determined structures of subtilisin Calsberg (Neidhart & Petsko, 1988) and the subtilisin–eglin C complex (Bode et al., 1986). The rotation function was dominated by two very strong peaks (Euler angles α = 169°, β = 128°, γ = 100° and α = 148°, β = 59°, γ = 154°). The value of the rotation function at the next highest peak was less than 60% of the value at the two highest peaks. The orientations indicated by the two peak values are related by an operation which is consistent with the strongest general (noncrystallographic) peak in the self-rotation function. Crowther–Blow translation functions calculated for each of the predicted orientations

Table II: Final Refinement Statistics for Selenosubtilisin Obtained with the Simulated Annealing Program XPLOR[a]

no. of rounds	5
resolution range (Å)	8.0–2.0
no. of reflections	25509
no. of reflections >2.0σ	22155
no. of protein atoms	3844
no. of calcium atoms	4
no. of solvent molecules	121
R-value[b] [40.0–2.0 Å, no $I/\sigma(I)$ cutoff]	0.209
R-value[b] [8.0–2.0 Å, $I/\sigma(I) > 2.0$]	0.173
rms deviations from ideal values	
bond length (Å)	0.015
bond angle (deg)	2.8
dihedral angle (deg)	25.1
improper angle (deg)	1.4

[a] The "cooling method" protocol was employed. [b] $R = \Sigma\|F_o\|-|F_c\|/\Sigma|F_o|$.

provided clear indication for the positions of the two molecules in the asymmetric unit: the value of the next highest peak in each of the intermolecular translation vector searches was below 85% of the height of the highest peak. The positions and orientations of the molecules were refined using the RMINIM routine in MERLOT. At this point the crystallographic residual R (where $R = \Sigma\|F_o|-|F_c\|/\Sigma|F_o|$) was 0.356.

Structure Refinement. Phases for the selenosubtilisin structure were calculated by placing the subtilisin model from the refined subtilisin–eglin C complex (Bode et al., 1986, 1987) in the two orientations and positions described above, and the structure was refined using the program XPLOR (Brunger et al., 1987) with data from 8.0- to 2.0-Å resolution. In the initial cycles of refinement all data within the indicated resolution range were included. In the final stages only those reflections for which $I/\sigma(I) > 2$ were included. Initial rigid body refinement reduced the crystallographic residual minimally (from 0.355 to 0.351). Subsequent full atomic positional refinement using the slow cool simulated annealing protocol (Brunger et al., 1990) resulted in a substantial improvement in the agreement between the observed and calculated structure factors [R = 0.272 for all data with $I/\sigma(I) > 2$]. At this stage a difference electron density map clearly indicated that the hydroxyl oxygen of serine 221 in both molecules in the asymmetric unit had been replaced by a seleninic acid moiety. The seleninic acid side chain was built into the map on the basis of the structure of (2-aminoethyl)seleninic acid (Karle & Estlin, 1969) obtained from the Cambridge Data Base. Subsequent refinement of positional and thermal parameters reduced the crystallographic residual to 0.218. At this point a complete atomic model was rebuilt into a series of "omit maps". In each omit map approximately 10% of the structure was deleted from the model prior to structure factor calculation, and the model for the deleted residues was rebuilt using maps calculated with coefficients of the type $(2F_o - F_c)$, α_c and $(F_o - F_c)$, α_c, where F_o are the observed amplitudes and F_c and α_c are the amplitudes and phases calculated from the model missing the omitted residues. The model was then refined with three rounds of refinement of positional and thermal parameters, alternating with manual rebuilding into omit maps, resulting in a reduction of the crystallographic residual to 0.208. Finally, solvent atoms were placed in difference maps, and the final model, including 121 water molecules and 4 calcium ions, was refined to convergence. The final statistics for the refined model are summarized in Table II.

Molecular Modeling and Molecular Dynamics. Molecular modeling experiments were carried out with the Insight II (2.1.0) and Discover (2.8) packages (Biosym Inc.). The relevant Sec221/Ser221 side chains were manually built into the selenosubtilisin and subtilisin Carlsberg active sites, respectively. The force field parameters for a disulfide bond were reparametrized to reflect the increased bond length and van der Waals radius of selenium as compared to sulfur in the selenenyl sulfide derivative. The resulting structures were subjected to 100 cycles of energy minimization to eliminate bad contacts and then subjected to molecular dynamics using simulated annealing methods. The structures were heated to 900 K, maintained at that temperature for 2 ps, and then slowly cooled to 200 K in 25° steps of 2-ps duration. During the dynamics runs, all the residues except the modified Sec221 or Ser221 were kept fixed. After dynamics, all constraints on the protein were relaxed, and the energy of the whole structure was minimized.

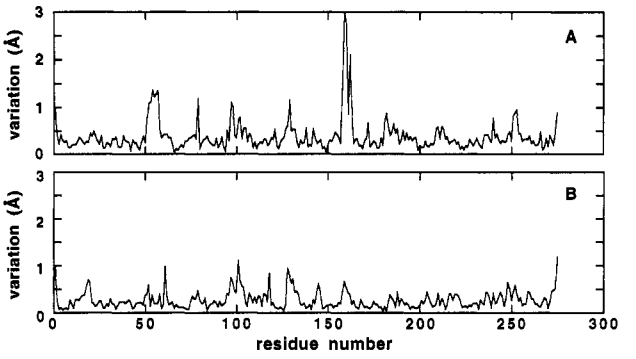

FIGURE 1: Comparison of the Cα positions of selenosubtilisin and free (A) or eglin C-bound (B) subtilisin Carlsberg.

RESULTS AND DISCUSSION

Overall Structure. Subtilases constitute a distinct family of serine proteases isolated originally from bacteria (Siezen et al., 1991). Subtilisin Carlsberg from *Bacillus licheniformis*, a subtilase of considerable commercial importance as an additive in washing detergents, was used as the template for the construction of selenosubtilisin. Its structure has been determined to high resolution in several laboratories, both as a complex with the protease inhibitor eglin C (Bode et al., 1986, 1987; McPhalen & James, 1988) and in the unliganded native state (Neidhart & Petsko, 1988). These structures differ from each other only in minor details and have the same overall topology as subtilisin BPN′ (Wright et al., 1969), another well-studied member of the subtilase family. They each have a characteristic core α/β protein scaffold and a catalytic triad consisting of residues Ser221, His64, and Asp32, spatially arranged like the analogous residues in the trypsin-like serine proteases which are evolutionarily unrelated to the subtilisins.

The structure of selenosubtilisin[2] is very similar to that of subtilisin Carlsberg. Least-squares superposition of all the equivalent α-carbon atoms of the selenoenzyme and the free and liganded forms of native subtilisin gave overall rms deviations of 0.5 and 0.3 Å, respectively. A plot of the distance between equivalent α-carbon positions as a function of residue number is shown in Figure 1. The most significant differences

[2] The structures of both selenosubtilisin molecules in the asymmetric unit were built and refined independently. Least-squares alignment of the two structures gave an overall rms deviation of 0.3 Å for equivalent α-carbon positions. The largest differences were observed for residues 97–100, which are completely disordered in molecule 2 and exhibit only weak electron density in molecule 1. For simplicity, only molecule 1 has been used for comparison with published subtilisin structures.

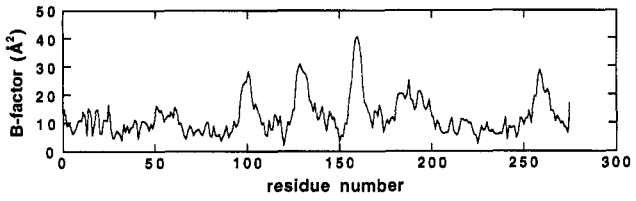

FIGURE 2: Average main-chain *B*-factors of selenosubtilisin (molecule 1) plotted as a function of residue number. The three regions with the highest average temperature factors correspond to surface loops.

between selenosubtilisin and the unliganded protease occur in the surface loops corresponding to residues 51–62 and 156–163. The region 51–62 of native subtilisin was reportedly characterized by weak electron density (Neidhart & Petsko, 1988), but the same residues in selenosubtilisin are well ordered and have relatively low *B*-factors (Figure 2) due to hydrogen bond contacts with a symmetry-related molecule. In the complex of subtilisin with eglin C (Bode et al., 1987), this loop is also well-defined and adopts the same backbone conformation as in the selenium derivative. Residues 156–163, on the other hand, have higher average *B*-factors and are less well packed with respect to the symmetry-related molecule. The observed changes in the conformation of this loop compared with unliganded subtilisin are presumably attributable to differences in crystal packing as well as to the intrinsic mobility of these residues. Again, the backbone conformation of selenosubtilisin's polypeptide chain in this region is similar to that seen in the subtilisin–eglin C complex.

The protein segment consisting of residues 97–103 is also of interest due to its proximity to the active site and because of the suggestion that its flexibility facilitates substrate and inhibitor binding through an induced-fit mechanism (Bode et al., 1987; Neidhard & Petsko, 1988). In selenosubtilisin, the main chain connecting these residues is displaced by approximately 1 Å from its position in the subtilisin–eglin C complex in a direction away from the active site. Although only one conformation is observed for the loop, the relatively high *B*-factors for residues 97–103 (~25 Å²) provide additional evidence for the mobility of this region in the absence of bound ligands.

The crystal structure of selenosubtilisin confirms that the selenium prosthetic group is incorporated site-selectively into the side chain of residue 221. The enzyme was chemically oxidized with hydrogen peroxide prior to crystallization in order to convert the selenium moiety to a single oxidation state. From the shape of the density and the interactions with surrounding residues (Figure 3), it appears that the side chain is present as a seleninic acid derivative ($ESeO_2H$), in agreement with independent chemical and spectroscopic evidence (House et al., 1992; Bell et al., 1993). As high concentrations of hydrogen peroxide are known to inactivate native subtilisin by oxidizing Met222 to the corresponding methionine sulfoxide (Stauffer & Etson, 1969), it was also of interest to ascertain the oxidation state of this residue. Evidence for partial oxidation of Met222 was provided by the ^{77}Se-NMR spectrum of the oxidized enzyme which showed two ^{77}Se resonances at 1188 and 1190 ppm (House et al., 1992). Although structural studies of peroxide-inactivated subtilisin BPN′ indicate that the sulfoxide oxygen would significantly alter the electronic microenvironment of the active site of the selenoenzyme by pointing directly toward the seleninic acid moiety (Bott et al., 1988), the resolution of our X-ray map precludes definitive clarification of this issue for selenosubtilisin. Examination of the $2F_o - F_c$ map at the 2σ level, however, shows qualitatively that a sulfoxide group can be accommodated in the electron density around Sδ of Met222. By this criterion, Met124, which is known to be susceptible to hydrogen peroxide (Bott et al., 1988), may also be partially oxidized. Additional density was not detected in the vicinity of Sδ of any of the other methionines in the structure, nor was evidence obtained for oxidation of any other protein residue, including tyrosines or tryptophans.

Bivalent cations are known to stabilize subtilisins against autolytic digestion, and two sites were found in selenosubtilisin that are probably occupied by calcium ions. Although calcium was not added to the crystal growth solutions, the enzyme was chemically modified in buffer containing 10 mM $CaCl_2$, and the calcium presumably copurified with it. The cation binding sites that we observed are the same as those previously identified by Bode et al. (1987) in the high-resolution structure of subtilisin Carlsberg. The high-affinity site defined by the loop formed by residues 75–81 appears to be fully occupied. The bound calcium ion is well ordered (temperature factor ≈6 Å²) and is surrounded by an octahedral coordination sphere of protein ligands, as previously described (Bode et al., 1987). The second site, in the vicinity of Tyr171, has been proposed to have lower affinity for calcium and appears to be only about 50% occupied in selenosubtilisin. It is also possible that a cation of lower electron density binds to this site, as suggested by McPhalen and James (1988). We find no convincing evidence for occupancy of a third calcium binding site formed by the 35–44 loop. Because the calcium binding sites are distant from the active site and because calcium binding does not adversely affect subtilisin's activity, the cations bound to selenosubtilisin are unlikely to alter its redox properties.

Internal solvent structure is a sensitive indicator of structural change. It is therefore notable that the distribution of ordered water molecules in selenosubtilisin is very similar to that in native subtilisin and the eglin C–subtilisin complex. A buried water that is hydrogen bonded to Asp32 and Asn123 is observed in all three structures. In addition, ordered water molecules in a crevice close to Leu75, near the high-affinity calcium binding site, and a chain of water molecules that stretches from the N-terminus of the protein to the side chains of His67 and Thr71 are conserved.

Catalytic Center. Except for the replacement of the alcohol side chain of Ser221 with the seleninic acid moiety of Sec221, the essential features of the subtilisin active site are preserved in selenosubtilisin. This is shown in Figure 4 where key residues in the respective binding pockets are superimposed.

The side chain of Sec221 has a single well-defined conformation in the modified protein. Its χ_1 torsional angle of −45° can be compared to the value of −136° observed for Ser221 in native subtilisin. The 90° rotation about the selenocysteine Cα–Cβ bond allows the seleninic acid side chain to adopt a low-energy staggered conformation. It also has the effect of moving the selenium atom away from the imidazole ring of His64 and closer to the oxyanion hole. As a result, energetically favorable hydrogen bonds can be made between Sec221 Oδ2 and the side-chain amide of Asn155 and the backbone amide of Sec221 (2.7 and 3.0 Å, respectively). This arrangement places the second seleninic acid oxygen atom, Oδ1, within hydrogen-bonding distance of Nε2 of His64 (2.8 Å), although the Oδ1 H–Nε2 hydrogen bond would have a distinctly nonlinear geometry.

^{77}Se-NMR spectroscopic studies of selenosubtilisin showed that the seleninic acid has a pK_a value that is at least 1.5 pH units lower than that of simple alkylseleninic acids and is consequently deprotonated above pH 4 (House et al., 1992). The hydrogen bonds from the oxyanion binding site must

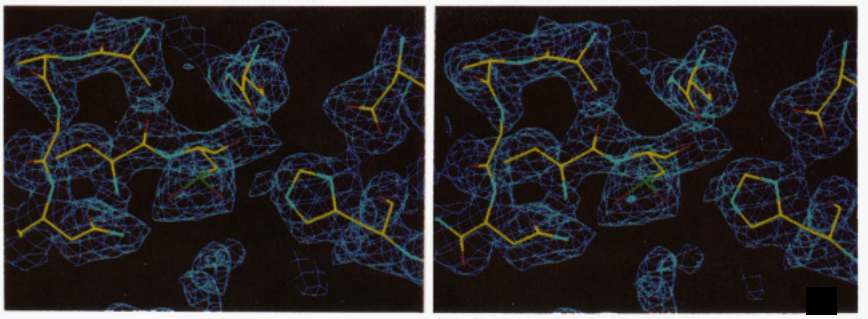

FIGURE 3: Difference Fourier omit map ($F_o - F_c$) of the active site of selenosubtilisin. The map was constructed with 10.0–2.0-Å data, contoured at 2σ, and displayed as a stereoview using a Silicon Graphics Crimson workstation with the program FRODO (Jones, 1978). The view is centered at the catalytic residue Sec221 and shows the hydrogen-bonding network extending from Asn155 in the oxyanion binding site (lower left), through the seleninic acid side chain of Sec221, to His64 and Asp32 (upper right).

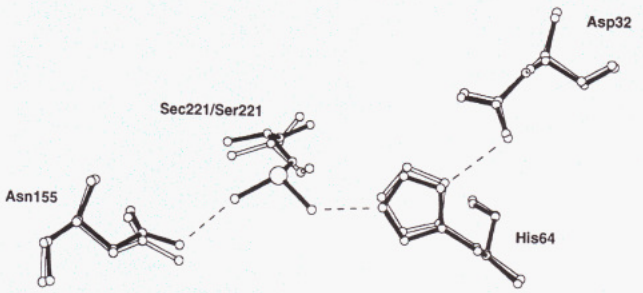

FIGURE 4: Superposition of the four active site residues (Asn155, Sec221/Ser221, His64, and Asp32) of selenosubtilisin and native subtilisin Carlsberg (Bode et al., 1987). The Cα coordinates for native subtilisin were superimposed onto the Cα coordinates of selenosubtilisin using the program OVRLAP (Rossman & Argos, 1975). The solid lines correspond to selenosubtilisin; the open lines are native subtilisin. The view is essentially the same as that illustrated in Figure 3.

contribute substantially to the observed stabilization of the seleninate form of the enzyme ($ESeO_2^-$). As the active site histidine remains protonated at least to pH 10, as judged by ^{1}H-NMR (House et al., 1993), it will also favor the conjugate base of the prosthetic group electrostatically, as will the macrodipole of the α-helix at whose N-terminus Sec221 is located. Native subtilisin exploits analogous interactions to stabilize the negatively charged tetrahedral intermediates and transition states that form during peptide hydrolysis (Robertus et al., 1972; Matthews et al., 1975).

Although seleninic acids with β-hydrogens readily decompose by *syn* elimination (Reich & Jasperse, 1987), selenosubtilisin is stable for many months when stored at 4 °C. The structural data show that the orientation of the enzyme-bound seleninate is not appropriate for an elimination reaction, which would require a planar arrangement of Cα–H, Cα, Cβ, Se, and either of the seleninic acid oxygen atoms. The strong hydrogen bonds that lock the seleninic acid into place in the folded protein would not be expected to be maintained in the unfolded state, and it was found experimentally that denaturation of the enzyme leads to rapid loss of selenium (House et al., 1992).

Incorporation of the seleninic acid moiety into the subtilisin binding pocket causes only modest adjustments in the orientations of the other active site residues. Thus, a 12° rotation around the Cβ–Cγ bond of Asn155 yields a more linear hydrogen bond between the side-chain amide and Oδ2 of the seleninic acid, and the plane of the imidazolium ring of His64 shifts 0.3–0.4 Å relative to its position in unmodified subtilisin Carlsberg, placing Nε2 in a better orientation for interaction with Sec221 Oδ1. The interactions between the imidazolium ring and the carboxylate side chain of Asp32, on the other hand, are unchanged in the modified active site. As part of the canonical catalytic triad, Asp32 helps to orient His64 by accepting a hydrogen bond from Nδ1 (Wright et al., 1969). Its carboxylate side chain appears to make the same contacts in selenosubtilisin as in native subtilisin, forming a hydrogen bond to the backbone amide of Thr33 in addition to its interaction with the catalytic histidine.

Correlation of Selenosubtilisin's Structure and Activity. The crystallographic data on selenosubtilisin provide a sound structural basis for interpreting the chemistry of the enzyme-bound seleninic acid. Like other seleninic acids (Kice & Lee, 1978), oxidized selenosubtilisin reacts with 3 equiv of thiol to give a selenenyl sulfide adduct plus a molecule of free disulfide (Wu & Hilvert, 1989; Bell et al., 1993). However, the enzyme is reduced by 3-carboxy-4-nitrobenzenethiol roughly 10^2 times more slowly than model alkylseleninic acids. Both processes are acid catalyzed, and an inflection was observed in the pH–rate profile of the model reaction at the pK_a of the seleninic acid (Bell et al., 1993). A corresponding inflection was not seen in the case of the enzyme between pH 4 and pH 8. These results suggest that protonation of the seleninate facilitates attack of the thiolate anion and that the decreased reactivity of oxidized selenosubtilisin toward thiols is largely due to the stability of its prosthetic group's conjugate base. Steric constraints imposed by the substrate binding pocket may also impede the reaction to some extent. The hydrophobic P1 specificity pocket, which normally accommodates the apolar side chain of the S1 amino acid in peptides cleaved by native subtilisin, is the most likely binding site for the aromatic thiol substrate used as the electron donor in these experiments. While thiols occupying this pocket probably have the best orientation for attacking the seleninic acid, an optimal reaction trajectory is precluded by the conformation of the Sec221 side chain.

Despite its relatively sluggish stoichiometric reaction with thiols, selenosubtilisin is a much better catalyst for the reduction of alkyl hydroperoxides by 3-carboxy-4-nitrobenzenethiol under turnover conditions than are model alkylselenium compounds (Wu & Hilvert, 1990; Bell et al., 1993). The main catalytic cycle is believed to involve interconversion of selenol, selenenic acid, and selenenyl sulfide intermediates (Scheme I). In this mechanism, oxidation of the prosthetic group to the seleninic acid is an unproductive side reaction that only becomes important at very high peroxide concentrations. Kinetic evidence suggests that the selenenyl sulfide is the predominant species under steady-state conditions and that its reduction is the rate-determining step in turnover catalysis (Bell et al., 1993).

The selenosubtilisin-catalyzed reduction of *tert*-butyl hydroperoxide by 3-carboxy-4-nitrobenzenethiol is at least 3

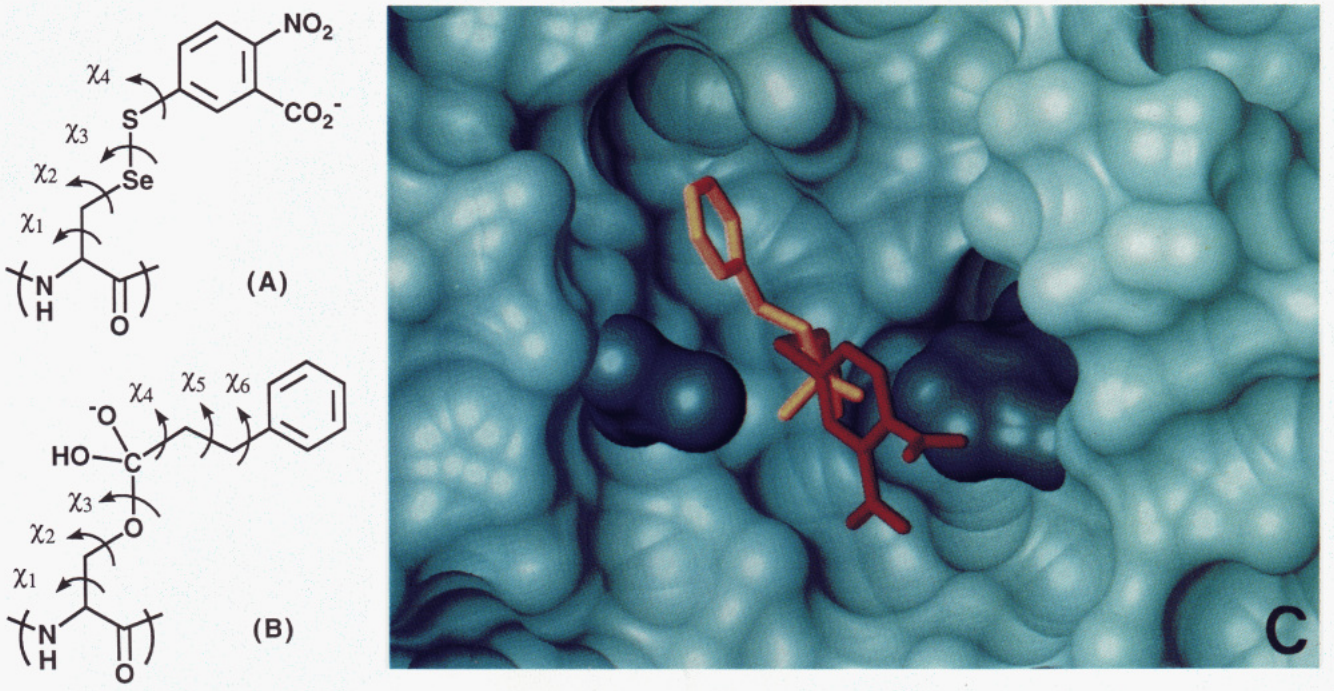

FIGURE 5: (A) The Sec221 selenenyl 3-carboxy-4-nitrophenyl sulfide derivative of selenosubtilisin, with the side-chain torsional angles, χ_1–χ_4, indicated. (B) The putative tetrahedral adduct that would result from addition of Ser221 of native subtilisin to 3-phenylpropionic acid, showing the side-chain torsional angles. (C) Final conformation of the selenenyl 3-carboxy-4-nitrophenyl sulfide group of selenosubtilisin (red) and the 3-phenylpropionic acid adduct of native subtilisin Carlsberg (yellow) in the superimposed active sites of the respective enzymes obtained after molecular dynamics and energy minimization of each structure, as described in the text. The solvent-accessible surface, shown in pale blue, was characterized for native subtilisin Carlsberg (after removal of the side chain of active site residue Ser221) with a probe of 1.7-Å radius using the programs AMS (Connolly, 1983) and MCS (Connolly, 1985). The active site residues Asn155 and His64 are shown in more saturated color than the rest of the protein. The enzyme is oriented as shown in Figure 4 with Asn155 to the left of residue 221 and His64 to its right. Note that the phenylpropionate side chain sits in the P1 specificity pocket. The shallow depression below residue 221 at the bottom of the figure is the P1′ binding site.

orders of magnitude faster than the corresponding reaction promoted by simple alkylseleninic acids, but it is unlikely that this combination of substrates is optimal for the enzyme. Indeed, a poor match between substrate and enzyme active site may account, in part, for the relative inefficiency of selenosubtilisin compared with glutathione peroxidase, which operates at rates near the diffusion limit. For optimal peroxidase activity, the thiol and peroxide substrates must be able to take full advantage of the active site geometry and binding specificity of the protein template. We anticipate that molecular modeling of the covalent intermediates and Michaelis complexes that occur along the reaction coordinate will facilitate the search for more appropriate substrate molecules for the semisynthetic peroxidase.

In an attempt to understand subtilisin's peroxidase activity with 3-carboxy-4-nitrobenzenethiol, we have used a molecular dynamics simulation to identify reasonable conformations of the corresponding enzyme-bound selenenyl sulfide derivative (Figure 5A). The aromatic side chain was initially placed in three topologically distinct locations, corresponding roughly to the P1 specificity pocket, the extended cleft in which the backbone of peptide substrates bind, and the P1′ leaving group site. After energy minimization, each conformation served as an independent starting point for a molecular dynamics experiment. All protein residues except Sec221 were fixed during the simulated annealing procedure, and upon completion of a run, the energy of the entire structure was minimized again to eliminate any bad contacts. The results of the three separate experiments showed convergence to a single conformation in which the side chain of Sec221 (torsion angles $\chi_1 = -68°$, $\chi_2 = 116°$, $\chi_3 = 74°$, and $\chi_4 = -77°$) is found near His64, with the plane of the 3-carboxy-4-nitrophenyl aromatic ring oriented roughly perpendicular to that of the imidazole ring (Figure 5C). This result is thus consistent with experimental evidence for an interaction between the selenenyl sulfide side chain and His64 deduced from the pH dependence of the ^{1}H-NMR resonances of the imidazolium Nδ1 and Nϵ2 protons (House et al., 1993).

As a control experiment, we modeled the tetrahedral adduct resulting from addition of native subtilisin's Ser221 to 3-phenylpropionic acid (Figure 5B) in an analogous manner. In this case, molecular dynamics yielded a final structure in which the Oδ1 and Oδ2 atoms of the covalent adduct are hydrogen bonded to Asn155 and to protonated His64 (3.0 and 2.9 Å, respectively), and the phenyl side chain remains bound in the apolar P1 specificity pocket ($\chi_1 = -61°$, $\chi_2 = 127°$, $\chi_3 = -164°$, $\chi_4 = 64°$, $\chi_5 = 168°$, and $\chi_6 = -62°$; see Figure 5C). The observed conformation is similar to that found crystallographically for the isosteric 2-phenylethaneboronic acid adduct of subtilisin BPN′ (Matthews et al., 1975). The boronate derivative is believed to be an excellent mimic of the anionic tetrahedral intermediates and transition states that are formed in the course of peptide hydrolysis by the natural enzyme.

Although the conformation deduced for the selenenyl 3-carboxy-4-nitrophenyl sulfide derivative of selenosubtilisin will have to be confirmed crystallographically, the results of the molecular dynamics simulation suggest that the selenenyl sulfide is aligned for attack by a second thiol molecule approaching from free solution. The selenol, like the seleninic acid, is known to have an unusually low pK_a value from spectroscopic titration of its ^{77}Se resonance (House et al., 1992), and its departure from the selenenyl sulfide is expected to be facilitated by protonation of the active site histidine. The resulting selenolate–imidazolium ion pair is quite stable over the pH range 4–10 (House et al., 1992, 1993), and

protonation of an active site residue ($pK_a \approx 7$) has been shown to be necessary for efficient turnover catalysis (Bell et al., 1993). His64 is the most likely ionizable group in this context.

The pK_a value of the selenol at the active site of glutathione peroxidase is not known, but it is likely to be somewhat higher than that of the selenol in selenosubtilisin. The only interactions available for stabilizing the selenolate in the natural selenoenzyme include a favorable helix macrodipole and relatively weak hydrogen bonds to Nε2 of Trp158 and to Nε2 of Gln80 (3.4 and 3.3 Å, respectively) (Epp et al., 1983). Arg177, which will bear a full positive charge under physiological conditions, is more than 6 Å away from the prosthetic group and is probably involved in substrate binding. Thus, selenosubtilisin's low catalytic efficiency compared to glutathione peroxidase is probably not a consequence of its selenol being a poorer leaving group.

A more likely explanation for the differences in reactivity between the two enzymes involves the relative steric accessibility of their respective selenenyl sulfide intermediates. The structure of glutathione peroxidase's selenenyl sulfide is not precisely known, but a model for the covalent complex with glutathione has been proposed on the basis of weak electron density in a difference Fourier map (Epp et al., 1983). In this model, the ligand's γ-Glu and C-terminal carboxyl groups are fixed by salt bridges to Arg177 and Arg50, and the N-terminal amine forms a hydrogen bond to Gln140. These contacts expose the selenenyl sulfide linkage of the intermediate to attack by a second molecule of glutathione from solution. In contrast, direct in-line attack of an external thiol on selenosubtilisin's selenenyl sulfide appears to be partially obstructed by the side chain of Asn155, according to our molecular dynamics simulation. If this conclusion is correct, it should be possible to augment selenosubtilisin's peroxidase efficiency by replacing Asn155 with an amino acid with a less sterically demanding side chain. Such a substitution may raise the pK_a of the selenol somewhat but should not compromise the intrinsic reactivity of the selenenyl sulfide bond, as the selenolate leaving group would still be amply stabilized through favorable electrostatic interactions with His64 and the macrodipole of the active site helix.

A distinct binding site for the second equivalent of 3-carboxy-4-nitrobenzenethiol required for reduction of selenosubtilisin's selenenyl sulfide group is not evident from our modeling experiments, and it is possible that higher peroxidase efficiencies might also be attained with thiols that are able to form productive (ESeSR·HSR) complexes. Crystallographic studies of boronic acid adducts of subtilisin showed that two molecules of 2-phenylethaneboronic acid can bind simultaneously in the active site, one covalently and the other noncovalently, by taking respective advantage of binding interactions associated with the P1 specificity pocket and a nearby site believed to recognize the leaving group residue P1′ in a true polypeptide substrate (Matthews et al., 1975). The boronic acid moieties of the two inhibitors are proximal in the enzyme complex studied, interacting directly through a hydrogen bond. Analogous complexes might be formed at the active site of selenosubtilisin with a thiol having a suitably long side chain, such as 2-phenylethanethiol. Positioning the attacking thiol near the selenenyl sulfide moiety could then provide a substantial entropic advantage to the enzymic reaction.

Conclusion. The high-resolution structure of selenosubtilisin has allowed the properties of the artificial enzyme—from the unusually low pK_a values of its seleninic acid and selenol derivatives to its reactivity with thiols in the presence and absence of peroxide—to be rationalized in terms of specific molecular interactions. It has, moreover, confirmed the overall structural integrity of the modified binding pocket, demonstrating that chemical modification can be a viable and practical alternative to genetically based methods for creating highly specific protein variants, and provides a basis for optimizing the activity of the first-generation catalyst through further substrate and enzyme engineering. We anticipate that crytallographic analysis of additional oxidation states and various covalent adducts of selenosubtilisin, in conjunction with detailed spectroscopic and kinetic investigations, will help to refine and deepen our understanding of the structure–function relationships that characterize this artificial enzyme. Given increasing interest in the biochemistry of selenium and in naturally occurring selenoenzymes like glutathione peroxidase and glycine reductase (Stadtman, 1980, 1990), such studies will be important for clarifying how molecular environment influences the reactivity of the selenium prosthetic group.

ACKNOWLEDGMENT

We thank Enrico A. Stura for help with the crystallization of selenosubtilisin and David Case, Ian A. Wilson, Jairo H. Arevalo, and Robyn L. Stanfield for helpful discussions.

REFERENCES

Abrahmsén, L., Tom, J., Burnier, J., Butcher, K. A., Kossiakoff, A., & Wells, J. A. (1991) *Biochemistry 30*, 4151–4159.
Bell, I. M., Fisher, M. L., Wu, Z.-P., & Hilvert, D. (1993) *Biochemistry 32*, 3754–3762.
Bode, W., Papamokos, E., Musil, D., Seemueller, U., & Fritz, H. (1986) *EMBO J. 5*, 813–818.
Bode, W., Papamokos, E., & Musil, D. (1987) *Eur. J. Biochem. 166*, 673–692.
Bott, R., Ultsch, M., Kossiakoff, A., Graycar, T., Katz, B., & Power, S. (1988) *J. Biol. Chem. 263*, 7895–7906.
Brunger, A. T., Kuriyan, J., & Karplus, M. (1987) *Science 235*, 458–460.
Brunger, A. T., Krukowski, A., & Erickson, J. (1990) *Acta Crystallogr. A46*, 585–593.
Carson, M. (1987) *J. Mol. Graphics 5*, 103–106.
Connolly, M. L. (1983) *J. Appl. Crystallogr. 16*, 548–558.
Connolly, M. L. (1985) *J. Mol. Graphics 3*, 19–24.
Epp, O., Ladenstein, R., & Wendel, A. (1983) *Eur. J. Biochem. 133*, 51–69.
Fitzgerald, P. M. D. (1988) *J. Appl. Crystallogr. 21*, 273–278.
Flohé, L., Günzler, W., Jung, G., Shaich, E., & Schneider, F. (1971) *Hoppe-Seyler's Z. Physiol. Chem. 352*, 159–169.
Günzler, W. A., Vergin, H., Müller, I., & Flohé, L. (1972) *Hoppe-Seyler's Z. Physiol. Chem. 353*, 1001–1004.
House, K. L., Dunlap, R. B., Odom, J. D., Wu, Z.-P., & Hilvert, D. (1992) *J. Am. Chem. Soc. 114*, 8573–8579.
House, K. L., Dunlap, R. B., Odom, J. D., & Hilvert, D. (1993) *Biochemistry 32*, 3468–3473.
Howard, A. J., Gilliland, G. L., Finzel, B. C., Poulos, T. L., Ohlendorf, D. H., & Salemme, F. R. (1987) *J. Appl. Crystallogr. 20*, 383–387.
Jones, T. A. (1978) *J. Appl. Crystallogr. 11*, 268–272.
Karle, I. L., & Estlin, J. A. (1969) *Z. Kristallogr. 129*, 147–152.
Kice, J. L., & Lee, T. W. S. (1978) *J. Am. Chem. Soc. 100*, 5094–5102.
Ladenstein, R. (1984) *Pept. Protein Rev. 4*, 173–214.
Matthews, B. W. (1968) *J. Mol. Biol. 33*, 491–497.
Matthews, D. A., Alden, R. A., Birktoft, J. J., Freer, S. T., & Kraut, J. (1975) *J. Biol. Chem. 250*, 7120–7126.
McPhalen, C. A., & James, M. N. G. (1988) *Biochemistry 27*, 6582–6598.
Nakatsuka, T., Sasaki, T., & Kaiser, E. T. (1987) *J. Am. Chem. Soc. 109*, 3808–3810.
Neidhart, D. J., & Petsko, G. A. (1988) *Protein Eng. 2*, 271–276.

Philipp, M., & Bender, M. L. (1983) *Mol. Cell. Biochem. 51*, 5–32.

Reich, H. J., & Jasperse, C. P. (1987) *J. Am. Chem. Soc. 109*, 5549–5551.

Robertus, J. D., Kraut, J., Alden, R. A., & Birktoft, J. J. (1972) *Biochemistry 11*, 4293–4303.

Rossman, M. G., & Argos, P. (1975) *J. Biol. Chem. 250*, 7525–7532.

Siezen, R. J., de Vos, W. M., Leunissen, J. A. M., & Dijkstra, B. W. (1991) *Protein Eng. 4*, 719–737.

Stadtman, T. C. (1980) *Annu. Rev. Biochem. 49*, 93–110.

Stadtman, T. C. (1990) *Annu. Rev. Biochem. 59*, 111–127.

Stauffer, C. E., & Etson, D. (1969) *J. Biol. Chem. 244*, 5333–5338.

Wells, J. A., & Estell, D. A. (1988) *Trends Biochem. Sci. 13*, 291–297.

Wendel, A. (1980) in *The Enzymatic Basis of Detoxification* (Jakoby, W. B., Ed.) Vol. 1, pp 333–353, Academic Press Inc., New York.

Wright, C. S., Alden, R. A., & Kraut, J. (1969) *Nature 221*, 235–242.

Wu, Z.-P., & Hilvert, D. (1989) *J. Am. Chem. Soc. 111*, 4513–4514.

Wu, Z.-P., & Hilvert, D. (1990) *J. Am. Chem. Soc. 112*, 5647–5648.